

Oxidative Metal–Metal Bond Cleavage in $\text{Tp}_2\text{Ru}_2(\text{CO})_4$ (Tp = Hydridotris(pyrazolyl)borate)

Morten Sørli and Mats Tilset*,¹

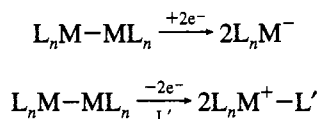
Department of Chemistry, University of Oslo, P.O. Box 1033 Blindern, N-0315 Oslo, Norway

Received February 9, 1995[⊗]

The Ru–Ru bonded dimer $\text{Tp}_2\text{Ru}_2(\text{CO})_4$ (**1**) is oxidized at $E^\circ = 0.15$ V vs $\text{Cp}_2\text{Fe}/\text{Cp}_2\text{Fe}^+$ in acetonitrile. The chemical or electrochemical 2-electron oxidation of **1** results in the formation of the solvent adducts $\text{TpRu}(\text{CO})_2(\text{Sol})^+$ (Sol: MeCN, **2**; THF, **3**; Me_2CO , **4**; H_2O , **5**). A derivative cyclic voltammetry investigation of the oxidation process has established that the metal–metal bond cleavage occurs from $\mathbf{1}^{*+}$ following the rate law $-\text{d}[\mathbf{1}^{*+}]/\text{d}t = k[\mathbf{1}^{*+}][\text{Sol}]$ (Sol = MeCN, THF, Me_2CO). An associative mechanism is furthermore implicated by large and negative entropies of activation. The rate of Ru–Ru bond cleavage is strongly solvent dependent and decreases in the order $\text{Me}_2\text{CO} > \text{MeCN} > \text{THF} > \text{CH}_2\text{Cl}_2$. The order of stabilities of the monomeric solvent adducts was established by observation of ligand-exchange reactions by ^1H NMR spectroscopy in nitromethane- d_3 , and the stabilities decrease in the order $\text{MeCN} > \text{H}_2\text{O} > \text{THF} > \text{Me}_2\text{CO}$.

Introduction

The oxidation and reduction of metal–metal bonded dimers, electronically saturated at both metals, constitute well-established procedures for the scission of metal–metal bonds. Such reactions provide cationic and anionic mononuclear species and have proven to be of great value in organometallic synthesis.²



The electrochemical oxidative and reductive cleavage reactions of group 6 dimers $\text{Cp}_2\text{M}_2(\text{CO})_6$ (in particular $\text{M} = \text{Mo}$, W)³ and group 8 dimers $\text{Cp}_2\text{M}_2(\text{CO})_4$ (mostly $\text{M} = \text{Fe}$, Ru)^{3a,b,e,4} have received special attention due to the widespread uses of such redox reactions in preparative organometallic chemistry. For these complexes, the incipient 1-electron oxidation and reduction intermediates undergo metal–metal bond cleavage by mechanisms that are only partially understood. Kinetic studies have indicated that, for $\text{Cp}_2\text{Fe}_2(\text{CO})_4$, the overall 2-electron oxidation and reduction reactions proceed by ECE mechanisms in which the cation radical^{4f} and anion radical,^{4c} respectively, rather than the dianions and dications, are the species which undergo metal–metal bond cleavage. Interestingly, whereas

$\text{Cp}_2\text{Fe}_2(\text{CO})_4$ contains bridging carbonyls in dichloromethane, the cation radical appeared to have semibridging CO ligands. The cleavage of $\text{Cp}^*\text{Fe}_2(\text{CO})_4^{*+}$ ($\text{Cp}^* = \eta^5\text{-C}_5\text{Me}_5$) was first-order with respect to $\text{Cp}^*\text{Fe}_2(\text{CO})_4^{*+}$ and first-order with respect to acetonitrile. A transient intermediate assumed to be $\text{Cp}_2\text{Fe}_2(\text{CO})_4(\text{NCMe})^{*+}$ was detected by cyclic voltammetry during the oxidation of $\text{Cp}_2\text{Fe}_2(\text{CO})_4$.^{4f}

Recently, the Tp (Tp = hydridotris(pyrazolyl)borate) and substituted derivatives have received considerable attention as ligands in organometallic and inorganic chemistry.⁵ The greater steric bulk and donor capability of this ligand, along with its tendency to enforce octahedral coordination geometry, impart significantly different properties and reactivities to structurally related Tp- and Cp-bonded species. For example, group 6 $\text{TpM}(\text{CO})_3^*$ radicals are monomeric in solution and in the solid state,⁶ whereas the Cp analogues form the metal–metal bonded dimers at near-diffusion-controlled rates for $\text{M} = \text{Mo}$ and W .⁷ The group 8 Tp carbonyl complex $\text{Tp}_2\text{M}_2(\text{CO})_4$, which has only terminal CO ligands, has been reported for $\text{M} = \text{Ru}$ ^{8a} but not for $\text{M} = \text{Fe}$ or Os . However, its chemistry has not yet been extensively explored.⁸ Except for the cleavage of the Ru–Ru bond in **1** by Br_2 or chlorinated solvents,^{8a} oxidative or reductive M–M bond cleavage reactions of such species have not yet been exploited for synthesis.

In this paper, we describe the oxidation chemistry of $\text{Tp}_2\text{Ru}_2(\text{CO})_4$ (**1**). The syntheses of the PF_6^- salts of the cationic solvent-coordinated complexes $\text{TpRu}(\text{CO})_2(\text{L})^+$ (L = acetonitrile, THF, acetone, water) are described, and a qualitative

[⊗] Abstract published in *Advance ACS Abstracts*, September 1, 1995.

- (1) Internet: mats.tilset@kjemi.uio.no.
- (2) (a) Collman, J. P.; Hegedus, L. S.; Norton, J. R.; Finke, R. G. *Principles and Applications of Organotransition Metal Chemistry*; University Science Books: Mill Valley, CA, 1987. (b) Wilkinson, G.; Stone, F. G. A.; Abel, E. W., Eds. *Comprehensive Organometallic Chemistry*; Pergamon: Oxford, U.K., 1982; Vols. 3, 4.
- (3) (a) Dessy, R. E.; Stary, F. E.; King, R. B.; Waldrop, M. *J. Am. Chem. Soc.* **1966**, *88*, 471. (b) Dessy, R. E.; Weissman, P. M.; Pohl, R. L. *J. Am. Chem. Soc.* **1966**, *88*, 5117. (c) Madach, T.; Vahrenkamp, H. *Z. Naturforsch., B: Anorg. Chem., Org. Chem.* **1979**, *34B*, 573. (d) Kadish, K. M.; Lacombe, D. A.; Anderson, J. E. *Inorg. Chem.* **1986**, *25*, 2246. (e) Pugh, J. R.; Meyer, T. J. *J. Am. Chem. Soc.* **1992**, *114*, 3784.
- (4) (a) Ferguson, J. A.; Meyer, T. J. *Inorg. Chem.* **1971**, *10*, 1025. (b) Miholova, D.; Vlcek, A. A., Jr. *Inorg. Chim. Acta* **1980**, *41*, 119. (c) Davies, S. G.; Simpson, S. J.; Parker, V. D. *J. Chem. Soc., Chem. Commun.* **1984**, 352. (d) Legzdins, P.; Wassink, B. *Organometallics* **1984**, *3*, 1811. (e) Hu, N.; Nie, G.; Jin, Z.; Chen, W. *J. Organomet. Chem.* **1989**, *377*, 137. (f) Bullock, J. P.; Palazatto, M. C.; Mann, K. R. *Inorg. Chem.* **1991**, *30*, 1284.

- (5) For an excellent and recent review, see: Trofimenko, S. *Chem. Rev.* **1993**, *93*, 943.
- (6) (a) Curtis, M. D.; Shiu, K.-B.; Butler, W. M.; Huffman, J. C. *J. Am. Chem. Soc.* **1986**, *108*, 3335. (b) Shiu, K.-B.; Lee, L.-Y. *J. Organomet. Chem.* **1988**, *348*, 357. (c) Kochi, J. K.; Bockman, T. M. *Adv. Organomet. Chem.* **1991**, *23*, 51. (d) MacNeil, J. H.; Watkins, W. C.; Baird, M. C.; Preston, K. F. *Organometallics* **1992**, *11*, 2761. (e) Skagestad, V.; Tilset, M. *J. Am. Chem. Soc.* **1993**, *115*, 5077. (f) Protasiewicz, J. D.; Theopold, K. H. *J. Am. Chem. Soc.* **1993**, *115*, 5559.
- (7) (a) Meyer, T. J.; Caspar, J. V. *Chem. Rev.* **1985**, *85*, 187 and references cited. (b) Scott, S. L.; Espenson, J. H.; Zhu, Z. *J. Am. Chem. Soc.* **1993**, *115*, 1789.
- (8) (a) Steyn, M. M. d. V.; Singleton, E.; Hietkamp, S.; Liles, D. C. *J. Chem. Soc., Dalton Trans.* **1990**, 2991. (b) Bruce, M. I.; Sharrocks, D. N.; Stone, F. G. A. *J. Organomet. Chem.* **1971**, *31*, 269. (c) Sun, N.-Y.; Simpson, S. J. *J. Organomet. Chem.* **1992**, *434*, 341.

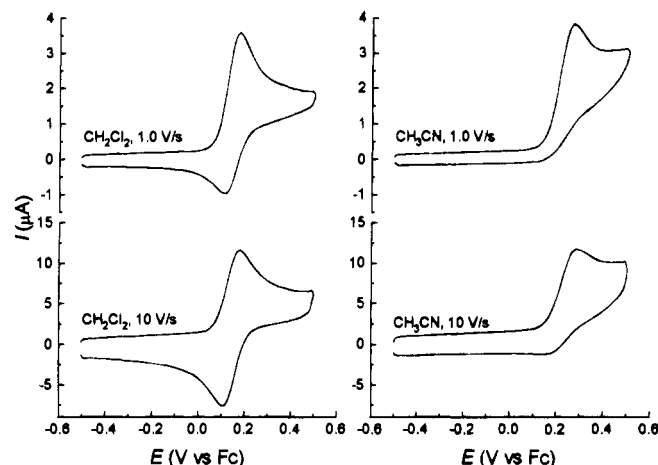


Figure 1. Cyclic voltammograms for the oxidation of $\text{Tp}_2\text{Ru}_2(\text{CO})_4$ (1.0 mM) in dichloromethane/0.2 M $\text{Bu}_4\text{N}^+\text{PF}_6^-$ and acetonitrile/0.1 M $\text{Bu}_4\text{N}^+\text{PF}_6^-$ at a Pt disk microelectrode ($d = 0.6 \text{ mm}$) at 20°C .

ordering of the stabilities of these complexes has been established by ligand-exchange reactions in nitromethane. The kinetics and mechanism of the oxidative cleavage of the Ru–Ru bond in different solvents have been investigated by electrochemical methods.

Results

I. Electrochemical Oxidation of $\text{Tp}_2\text{Ru}_2(\text{CO})_4$ (1). The initial investigation of the oxidation chemistry of **1** was done by cyclic voltammetry (CV). Figure 1 shows cyclic voltammograms for the oxidation of **1** in dichloromethane (left) and acetonitrile (right) at voltage sweep rates $\nu = 1.0 \text{ V/s}$ (top) and 10.0 V/s (bottom). In dichloromethane, **1** undergoes a nearly Nernstian electron transfer at $E^\circ = 0.15 \text{ V vs C}_2\text{P}_2\text{Fe/C}_2\text{P}_2\text{Fe}^+$ (Fc). (The E° value is taken to be the midpoint between the anodic and cathodic CV peaks.) The anodic to cathodic peak separation in this solvent was $\Delta E_p = 62 \text{ mV}$ at $\nu = 1.0 \text{ V/s}$ (cf. $\Delta E_p = 60 \text{ mV}$ for the $\text{C}_2\text{P}_2\text{Fe/C}_2\text{P}_2\text{Fe}^+$ couple under identical conditions). The cation radical $\mathbf{1}^{+\cdot}$ is relatively stable on the experimental time scale at this sweep rate, since the cathodic wave in the CV plot is almost, but not quite, as intense as the anodic wave.

In acetonitrile, the rate of the follow-up reaction that consumes $\mathbf{1}^{+\cdot}$ is even greater than in dichloromethane: the oxidation of **1** in acetonitrile is chemically irreversible at $\nu = 1.0 \text{ V/s}$ as indicated by the absence of a reduction peak during the negative-going reverse scan. This qualitatively shows that the rate of the reaction of $\mathbf{1}^{+\cdot}$ is highly sensitive to the nature of the solvent. Chemical reversibility was only in part restored at $\nu = 10 \text{ V/s}$. In THF/0.2 M $\text{Bu}_4\text{N}^+\text{PF}_6^-$, the extent of chemical reversibility was qualitatively found to be intermediate between that in dichloromethane and that in acetonitrile. In acetone/0.2 M $\text{Bu}_4\text{N}^+\text{PF}_6^-$, the rate of reaction of $\mathbf{1}^{+\cdot}$ was even greater than that in acetonitrile.

A plot of $I_p/\nu^{1/2}$ vs ν for the oxidation of **1** in acetonitrile (I_p = anodic peak current, corrected by subtraction of the non-Faradaic background) at 20°C at the Pt electrode showed the $I_p/\nu^{1/2}$ ratio to be independent of ν at $\nu > 2 \text{ V/s}$. Curvature was however seen at lower values for ν . At $\nu = 0.1 \text{ V/s}$, the ratio was 1.8 times that at high ν (lower ν values than 0.1 V/s were not checked because of the onset of significant contributions from spherical diffusion). A constant $I_p/\nu^{1/2}$ ratio was observed for the oxidation of ferrocene under identical conditions. These findings suggest⁹ that, on the time scale of the measurements, the oxidation is a 1-electron process (per dimer)

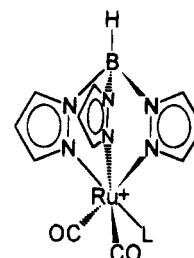
at high ν and a 2-electron process at low ν . Similar behavior was found in a study of the reductive cleavage of $\text{Cp}_2\text{Fe}_2(\text{CO})_4$.^{4c}

At $\nu = 1.0 \text{ V/s}$, no other oxidation waves were detected at potentials up to 1.5 V vs Fc . However, at $\nu > 25 \text{ V/s}$, a chemically irreversible, broad wave of relatively low intensity appeared with a peak potential of ca. 1.1 V vs Fc . We attribute this wave to the oxidation of $\mathbf{1}^{+\cdot}$ to $\mathbf{1}^{2+}$ which undergoes a rapid follow-up reaction, presumably a metal–metal bond cleavage. The reason that this wave was not observed at lower ν values is that, on the longer time scale, $\mathbf{1}^{+\cdot}$ has time to quantitatively react before the potential of the second wave is reached. Thus, the diffusion layer is essentially depleted of $\mathbf{1}^{+\cdot}$ and no signal can be seen. The separation between the two waves is large enough that the second oxidation process will not interfere in cyclic voltammetry experiments to be described later.

A reduction peak was observed at -2.15 V vs Fc during the reverse scan when **1** was oxidized in acetonitrile. The relative intensity of this peak was inversely dependent on the scan rate, indicating that the peak is due to the reduction of a product arising from $\mathbf{1}^{+\cdot}$. A comparison with an authentic sample (vide infra) established that the species giving rise to this peak was $\text{TpRu}(\text{CO})_2(\text{NCMe})^+$ (**2**). No other product peaks were seen, suggesting that CO-substitution reactions (i.e. leading to $\text{TpRu}(\text{CO})(\text{NCMe})_2^+$) do not occur.

Constant-potential coulometry measurements at the oxidation peak potential of **1** established that the oxidation of **1** was a 2-electron process (i.e., one electron per Ru center) in acetonitrile, THF, and acetone. Coulometry is a relatively slow technique, and therefore, this finding agrees with the results of the $I_p/\nu^{1/2}$ vs ν analysis. Analysis of the electrolysis products by ^1H NMR spectroscopy after exhaustive electrolyses and workup revealed the presence of the solvent adducts $\text{TpRu}(\text{CO})_2(\text{L})^+$ (L: MeCN, **2**; THF, **3**; Me₂CO, **4**). In acetone, the aqua complex (L = H₂O, **5**) was also generated along with **4**. Details of the independent syntheses and characterization of these species are given in the following.

II. Synthesis and Characterization of $\text{TpRu}(\text{CO})_2(\text{L})^+\text{PF}_6^-$. The solvent-coordinated complexes **2–4** were prepared by oxidation of **1** with 2 equiv of $\text{Cp}_2\text{Fe}^+\text{PF}_6^-$ in the appropriate solvent. Complete NMR and IR spectroscopic data for the new



L = MeCN (**2**), THF (**3**), Me₂CO (**4**), H₂O (**5**)

complexes are given in the Experimental Section. Table 1 shows partial ^1H NMR spectroscopic data, listing signals in the Tp region of the spectra, recorded in nitromethane-*d*₃. The ^1H NMR spectra of the products in all cases displayed six signals (1:1:1:2:2:2 relative ratios) that are attributed to the Tp ligands. This is consistent with a static structure with C_s symmetry, containing one unique and two identical (by virtue of the mirror plane bisecting the molecule) pyrazole rings. Structures with noninterchanging (on the NMR time scale) pyrazole rings have

(9) $I_p/\nu^{1/2}$ is independent of ν for a Nernstian 1-electron transfer.¹⁰
 (10) Bard, A. J.; Faulkner, L. R. *Electrochemical Methods. Fundamentals and Applications*; Wiley: New York, 1980.
 (11) Jiang, Z.; Sen, A. *Organometallics* **1993**, *12*, 1406.

Table 1. ^1H NMR Data for Oxidation Products $\text{TpRu}(\text{CO})_2(\text{L})^+$

| complex | ^1H NMR, δ (Tp region) (in nitromethane- d_3) |
|--|--|
| $\text{TpRu}(\text{CO})_2(\text{NCMe})^+ (2)$ | 6.43 (t, 1H), 6.50 (t, 2H), 7.90 (d, 1H), 7.95 (d, 1H), 7.99 (d, 2H), 8.10 (d, 2H) |
| $\text{TpRu}(\text{CO})_2(\text{THF})^+ (3)$ | 6.38 (t, 1H), 6.57 (t, 2H), 7.73 (d, 1H), 7.93 (d, 1H), 8.08 (d, 2H), 8.18 (d, 2H) |
| $\text{TpRu}(\text{CO})_2(\text{Me}_2\text{CO})^+ (4)$ | 6.44 (t, 1H), 6.50 (t, 2H), 7.85 (d, 1H), 7.93 (d, 1H), 8.01 (d, 1H), 8.03 (d, 2H) |
| $\text{TpRu}(\text{CO})_2(\text{H}_2\text{O})^+ (5)$ | 6.39 (t, 1H), 6.51 (t, 2H), 7.77 (d, 1H), 7.95 (d, 1H), 8.03 (d, 2H), 8.05 (d, 2H) |

been previously reported for $\text{TpRu}(\text{CO})(\text{PPh}_3)(\text{L})^+$ species,^{8c} as well as for **1**.^{8a}

$\text{TpRu}(\text{CO})_2(\text{NCMe})^+\text{PF}_6^-$ (**2**(PF_6^-)) was obtained in 60% yield from the oxidation of **1** in acetonitrile after recrystallization from acetonitrile/ether. Oxidation of **1** in THF led to the direct precipitation of $\text{TpRu}(\text{CO})_2(\text{THF})^+\text{PF}_6^-$ (**3**(PF_6^-)), isolated in 71% yield after recrystallization.

The oxidation of **1** in dry acetone yielded a solid that consisted mostly of $\text{TpRu}(\text{CO})_2(\text{OCMe}_2)^+\text{PF}_6^-$ (**4**(PF_6^-)), but the sample was always contaminated by 20–30% of the aqua complex $\text{TpRu}(\text{CO})_2(\text{H}_2\text{O})^+\text{PF}_6^-$ (**5**(PF_6^-)). The addition of a drop of D_2O to the NMR tube containing a mixture of **4**(PF_6^-) and **5**(PF_6^-) in nitromethane- d_3 rapidly converted **4** to $\text{TpRu}(\text{CO})_2(\text{D}_2\text{O})^+$ (**5**- d_2), as evidenced by the changes in the Tp region of the ^1H NMR spectrum. Attempts at obtaining pure **4** by displacement of THF from **3** with dry acetone likewise invariably resulted in a mixture of **4** and **5**. The $^{13}\text{C}\{^1\text{H}\}$ spectrum of **4** displayed a resonance due to CO at δ 193.7 and one due to coordinated acetone at δ 205.6; the high-field value of the latter strongly suggests an η^1 , terminal bonding mode of the acetone ligand, rather than an η^2 , side-on bonded ligand which would give rise to a signal at much lower field.¹²

Oxidation of **1** with 2 equiv of $\text{Cp}_2\text{Fe}^+\text{PF}_6^-$ in a two-phase, 1:1 mixture of dichloromethane and water resulted in **5**(PF_6^-). The H_2O resonance could not be detected in nitromethane- d_3 , possibly due to H/D exchange with the relatively acidic solvent or residual D_2O contained in the solvent. The ^1H NMR data for the isolated complex completely matched those of the side product from the oxidation of **1** in acetone.

A comparison of IR ν_{CO} and oxidation potential data for $\text{TpM}(\text{CO})_3^-$ and $\text{CpM}(\text{CO})_3^-$ ($\text{M} = \text{Cr}, \text{Mo}, \text{W}$) showed that the Tp anion acts as a better donor than the Cp anion.^{6e} Interestingly, the same conclusion cannot be drawn from a comparison of IR ν_{CO} data (dichloromethane) for $\text{TpRu}(\text{CO})_2(\text{NCMe})^+$ (2040, 2090 cm^{-1}) vs $\text{CpRu}(\text{CO})_2(\text{NCMe})^+$ (2025, 2070 cm^{-1}). It is noteworthy that, also previously, some (but not all) $\text{TpRu}(\text{CO})(\text{PPh}_3)(\text{L})^+$ complexes have been found to exhibit IR ν_{CO} bands at higher energies than the $\text{CpRu}(\text{CO})(\text{PPh}_3)(\text{L})^+$ analogues.^{8c} The reason for this rather surprising difference between the isoelectronic group 6 anions and the Ru cationic complexes is not apparent. The steric bulk of the acetonitrile ligand should be comparable to that of CO, so steric perturbations of the coordination geometry can be ruled out.

III. Derivative Cyclic Voltammetry Investigation of the Oxidative Ru–Ru Bond Cleavage in **1.** The details of the oxidative cleavage of **1** were probed by derivative cyclic voltammetry (DCV).¹³ The application of DCV in organometallic chemistry has been previously described in detail,¹⁴ so

(12) Méndez, N. Q.; Seyler, J. W.; Arif, A. M.; Gladysz, J. A. *J. Am. Chem. Soc.* **1993**, *115*, 2323.

(13) (a) Ahlberg, E.; Parker, V. D. *J. Electroanal. Chem. Interfacial Electrochem.* **1981**, *121*, 73. (b) Parker, V. D. *Acta Chem. Scand., Ser. B* **1984**, *B38*, 165. (c) Parker, V. D. *Electroanal. Chem.* **1986**, *14*, 1.

(14) (a) Tilset, M.; Bodner, G. S.; Senn, D. R.; Gladysz, J. A.; Parker, V. D. *J. Am. Chem. Soc.* **1987**, *109*, 7551. (b) Aase, T.; Tilset, M.; Parker, V. D. *J. Am. Chem. Soc.* **1990**, *112*, 4974. (c) Tilset, M. In *Energetics of Organometallic Species*; Simões, J. A. M., Ed.; Kluwer Academic: Dordrecht, The Netherlands, 1992; p 109. (d) Tilset, M.; Skagestad,

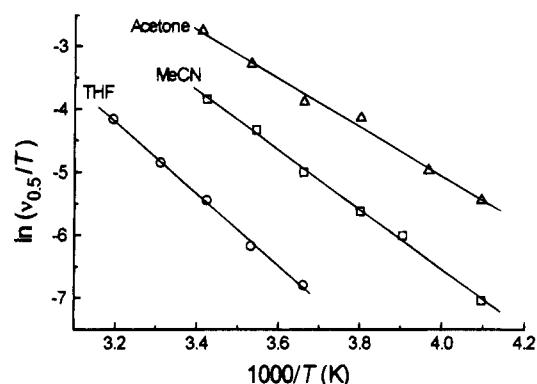


Figure 2. Arrhenius-type plot of $\ln(v_{0.5}/T)$ vs $1000/T$ for the reactions of 1^{+} in acetonitrile, THF, and acetone/ $\text{Bu}_4\text{N}^+\text{PF}_6^-$. $E_{\text{switch}} - E_{\text{rev}} = 200$ mV, 0.6 mm Pt disk electrode, 1.0 mM substrate.

only a brief summary of the method will be given in the following. In a DCV analysis of the mechanisms of electrode reactions, the voltage sweep rate ν is adjusted to ν_c at which the reverse to forward derivative peak current ratio, I_r/I_f , equals a constant value c . The separation between the CV switching potential, E_{switch} , and the reversible electrode potential for the process under investigation, E_{rev} , is maintained at a fixed value for a measurement series (chosen as 200 mV for the present work). The value of ν_c will clearly depend on the rate of disappearance of the electrode-generated intermediate. For example, for $I_r/I_f = 0.5$ one obtains $\nu_{0.5}$, which correlates inversely with the half-life of the electrode-generated species and directly with the rate constant for its disappearance. Measurements of ν_c under different experimental conditions provide information about the order of the homogeneous reaction with respect to substrate and other reactants, activation energies, etc. When the rate law and the stoichiometry of the reaction have been established, a comparison of ν_c data with theoretical working curves provides the actual rate constants for the reactions.¹³

A DCV reaction-order analysis in acetonitrile/0.1 M $\text{Bu}_4\text{N}^+\text{PF}_6^-$ established that $\nu_{0.5}$ was independent of the substrate concentration in the range 0.5–2.0 mM, implying a first-order reaction with respect to 1^{+} . The same situation pertained when the solvent/electrolyte was changed to THF/0.2 M $\text{Bu}_4\text{N}^+\text{PF}_6^-$ and to acetone/0.2 M $\text{Bu}_4\text{N}^+\text{PF}_6^-$. As suggested by a reviewer, complementary kinetic studies may be performed by monitoring the intensity of the reduction peak of $\text{TpRu}(\text{CO})_2(\text{NCMe})^+$ as a function of scan rate and substrate concentration. Unfortunately, complications believed to arise from adsorption at the electrode surface rendered this method less valuable for quantitative purposes.

Figure 2 shows Arrhenius-type plots of $\ln(v_{0.5}/T)$ vs $1/T$ from variable-temperature DCV measurements.¹⁵ By this treatment,

V.; Parker, V. D. In *Molecular Electrochemistry of Inorganic, Bioinorganic and Organometallic Compounds*; Pombeiro, A. J. L., McCleverty, J. A., Eds.; Kluwer Academic: Dordrecht, The Netherlands, 1992; p 267. (e) Smith, K.-T.; Rømming, C.; Tilset, M. *J. Am. Chem. Soc.* **1993**, *115*, 8681. (f) Pedersen, A.; Tilset, M. *Organometallics* **1993**, *12*, 56.

(15) Note that the $\ln(v_{0.5}/T)$ vs $1/T$ plots represent Arrhenius-type (and not Eyring) relationships.¹³

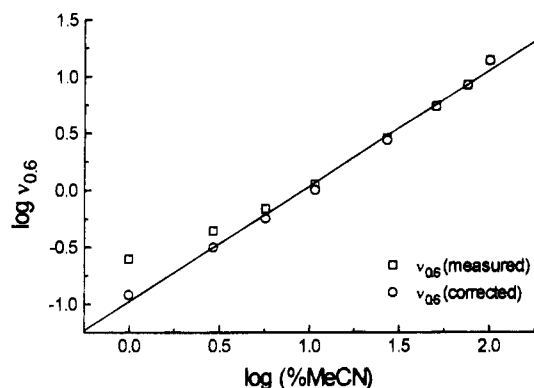


Figure 3. Dependence of $v_{0.6}$ on the volume fraction of acetonitrile for the reaction of 1^{*+} in dichloromethane/0.2 M $\text{Bu}_4\text{N}^+\text{PF}_6^-$ at 20 °C. $E_{\text{switch}} - E_{\text{rev}} = 200$ mV, 0.6 mm Pt disk electrode, 1.0 mM substrate. See text for explanation of the method of background correction.

the activation energy of the homogeneous chemical reaction can be determined without making a prior assumption of a specific reaction mechanism.¹³ The activation energies obtained from three independent measurement series for each solvent were as follows: acetonitrile, $E_a = 35(2)$ kJ/mol; THF, 44(2) kJ/mol; acetone, 31(1) kJ/mol.

Figure 3 shows the dependence of $v_{0.6}$ on $[\text{MeCN}]$ in dichloromethane/acetonitrile/0.2 M $\text{Bu}_4\text{N}^+\text{PF}_6^-$ mixtures at constant substrate concentration. Since $v_{0.6}$ is proportional to the macroscopic rate constant k_{obs} , a simple rate law of the type $\text{rate} = -d[1^{*+}]/dt = k_{\text{obs}}[1^{*+}]$ should give a straight line with a slope of unity for $\log v_{0.6}$ vs $\log [\text{MeCN}]$. A somewhat curved plot with slope 0.87(0.05) (circles, Figure 3) is obtained. A likely reason for the curvature is that the reaction of 1^{*+} proceeds at a slow but measurable rate even in dichloromethane; the contribution of this "background reaction" is most strongly felt at low $[\text{MeCN}]$. In an attempt at correcting for this background reaction, the contribution to the overall rate that is attributable to the background reaction (=volume fraction dichloromethane times $v_{0.6}$ as measured in dichloromethane alone) was subtracted from the measured $v_{0.6}$ values. While this procedure may be naively simple in that it assumes that the activity of the cosolvent is linearly dependent on its concentration, with complete neglect of solvent-cosolvent interactions, we nevertheless believe that the resulting data may quantitatively give a better picture of the true effect of the acetonitrile cosolvent on a molecular scale. Figure 3 (squares) shows the result, a straight line with slope of 1.01(0.03), in much better agreement with the expectations for a reaction that is first order with respect to $[\text{MeCN}]$.

The dependence of the reaction rate on $[\text{THF}]$ and on $[\text{acetone}]$ in dichloromethane was investigated by following the same procedure. Also in these cases, essentially linear plots with slopes closer to unity (slopes of 1.22(0.05) and 1.08(0.07), respectively) were obtained after correction for the background reaction. All these results are readily reconciled by a rate-limiting reaction between 1^{*+} and acetonitrile, THF, or acetone.

On the basis of the preparative results, it is evident that the kinetic data that were obtained for the reaction between 1^{*+} and acetone may actually be composite data arising from its reaction with acetone and from its reaction with inadvertent traces of water in the acetone. Attempts at quantifying the contribution from water by the intentional addition of controlled amounts of water to the electrolyte were unsuccessful due to inferior electrochemical response in the presence of water. It is therefore not clear whether the formation of **5** occurs in a competition between reactions of 1^{*+} with water and acetone or in a follow-up reaction between kinetically formed **4** and water.

IV. Mechanism of Oxidative Ru–Ru Bond Cleavage.

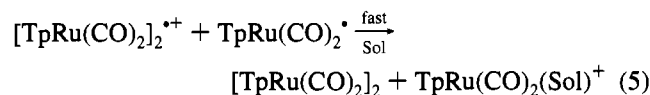
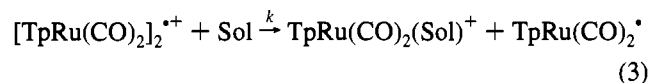
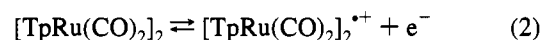
The combined electrochemical results provide detailed insight into the mechanism of the oxidative Ru–Ru bond cleavage. In particular, the decrease in $I_p/\nu^{1/2}$ corresponding to 1.8 electrons at 0.1 V/s to limiting 1 electron behavior at ν greater than 2 V/s suggests that rate-determining cleavage takes place after the transfer of one electron. The second electron is transferred after the rate-determining bond scission.

The DCV investigation of the oxidation of $[\text{TpRu}(\text{CO})_2]_2^{*+}$ in acetonitrile, THF, and acetone established the overall rate law of eq 1. Scheme 1 shows two possible reaction mechanisms

$$\text{rate} = -d[1^{*+}]/dt = k[1^{*+}][\text{Sol}] \quad (1)$$

that are in accord with the data. (Quite similar mechanisms were discussed in detail by Mann and co-workers^{4f} for the oxidative cleavage of $\text{Cp}_2\text{Fe}_2(\text{CO})_4$.) The initial step, the reaction of 1^{*+} with the solvent (Sol) (eq 3) generates the product $\text{TpRu}(\text{CO})_2(\text{Sol})^+$ along with the 17-electron radical $\text{TpRu}(\text{CO})_2^*$. This radical may proceed to the product by different mechanisms to be described in the following.

Scheme 1



In eq 4, the radical dimerizes to re-form **1**, which of course re-enters the scheme in reaction 2. The chemistry of the proposed radical $\text{TpRu}(\text{CO})_2^*$ has never been reported, but precedent for this type of behavior is found in the near-diffusion-controlled rates of dimerization of various $\text{CpM}(\text{CO})_x^*$ radicals.⁷ We concur that the dimeric species $\text{Tp}_2\text{M}_2(\text{CO})_6$ are unknown because the radicals $\text{TpM}(\text{CO})_3^*$ do not dimerize due to excessive steric crowding in the would-be dimers. Still, the mere existence of $\text{Tp}_2\text{Ru}_2(\text{CO})_4$ strongly suggests that dimerization of the hitherto unobserved radical $\text{TpRu}(\text{CO})_2^*$ may be a facile process.

Alternatively, the radical can be oxidized to give the product at a rate exceeding that of radical dimerization. This oxidation may occur either homogeneously by electron transfer to 1^{*+} to generate the product and re-form **1** (eq 5) or heterogeneously at the electrode surface. In either case, radical oxidation is likely facilitated by prior solvent coordination to give the more readily oxidized 19-electron radical $\text{TpRu}(\text{CO})_2(\text{Sol})^*$, paralleling the behavior of the radicals $\text{CpM}(\text{CO})_3^*$ ($\text{M} = \text{Mo}, \text{W}$) in acetonitrile.¹⁶ We consider that the heterogeneous radical oxidation option is unlikely on the ground that the cation radical 1^{*+} has a significant lifetime in solution; therefore, $\text{TpRu}(\text{CO})_2^*$ will be generated in the diffusion layer far away from the electrode surface. It follows that if the radical can undergo relatively rapid dimerization in the absence of 1^{*+} , then the eventual oxidation of the radical must occur homogeneously (with 1^{*+} as the oxidant) at a rate greater than the dimerization rate.

Before the experimental $v_{0.5}$ data can be converted to actual rate constants by comparison with theoretical working curves, one of the possible reaction mechanisms must be assumed. The

Table 2. Kinetic Data for the Reactions of $1^{+\bullet}$ ^a

| | acetonitrile ^b | THF ^c | acetone ^d |
|--|---------------------------|------------------|----------------------|
| ΔH^\ddagger , kJ/mol | 32.8 (1.2) | 41.2 (1.6) | 28.7 (1.1) |
| ΔS^\ddagger , J/(K·mol) | -86.1 (4.6) | -68.6 (5.4) | -90.0 (4.2) |
| $k(20^\circ\text{C})$, s ⁻¹ ^e | 282 | 74 | 897 |

^a By comparison of variable-temperature DCV data ($\nu_{0.5}$, $E_{\text{sw}} - E_{\text{rev}} = 200$ mV, 1.0 mM substrate) with theoretical data assuming the radical dimerization mechanism given by eqs 2–4. One standard error in parentheses. ^b 0.1 M $\text{Bu}_4\text{N}^+\text{PF}_6^-$, -30 to +20 °C. ^c 0.2 M $\text{Bu}_4\text{N}^+\text{PF}_6^-$, 0–40 °C. ^d 0.2 M $\text{Bu}_4\text{N}^+\text{PF}_6^-$, -30 to +20 °C. ^e Pseudo-first-order rate constants from interpolation of measured rate constants with the Eyring equation.

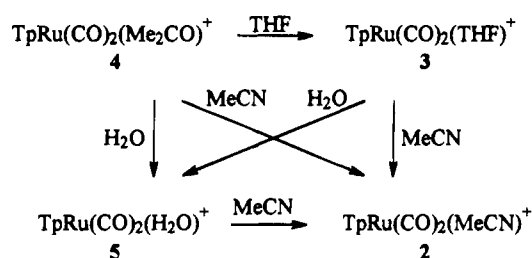
two alternative mechanisms, which differ in the fate of the $\text{TpRu}(\text{CO})_2^{\bullet}$ radical (homogeneous dimerization, eq 4, vs homogeneous oxidation, eq 5), cannot be distinguished on the basis of the data at hand. The experimental data have therefore been compared with theoretical working curves¹³ of $\ln c$ vs $\ln(k/a)$ (where c = derivative peak current ratio and $a = F\nu/RT$) for the two likely mechanisms for determination of the kinetic parameters $k(20^\circ\text{C})$, ΔH^\ddagger , and ΔS^\ddagger . The two mechanisms give slightly different values for ΔS^\ddagger , which is reflected in rate constants differing by a factor of 2. This difference stems from the fact that, in the radical dimerization mechanism (eqs 2–4), only one cation radical $1^{+\bullet}$ is consumed per solvent-induced cleavage (eq 3) whereas, in the radical oxidation mechanism (eqs 2, 3, 5), two cation radicals are consumed as a result of the rapid step (5).

The resulting kinetic parameters for the radical dimerization mechanism (eqs 2–4) are summarized in Table 2. For the radical oxidation mechanism, the rate constants will be half the values given, and the ΔS^\ddagger values will be 6.0 J/(K·mol) more negative. In either case, the ΔS^\ddagger values are clearly indicative of an associative reaction for the metal–metal bond cleavage of $1^{+\bullet}$. Associative pathways have been well established for ligand substitutions at mononuclear, 17-electron metal radicals, and the ΔS^\ddagger values for the reactions at $1^{+\bullet}$ are quite similar to those reported for such substitution reactions.¹⁷ Oxidation of $\text{Cp}_2\text{Fe}_2(\text{CO})_4$ provided the transient cation radical which underwent solvent-assisted cleavage, and oxidation of $\text{Cp}^*\text{Fe}_2(\text{CO})_4$ yielded solutions of the cation radical. A rate constant ($118 \text{ M}^{-1} \text{ s}^{-1}$) for the reaction of the latter with acetonitrile was reported,^{4f} but activation parameters were not reported.

The reactivity order of the solvents is $\text{Me}_2\text{CO} > \text{MeCN} > \text{THF}$. The rates correlate poorly with the donor numbers of the solvents ($\text{THF} > \text{Me}_2\text{CO} > \text{MeCN}$).¹⁸ The reactivity of solvent molecules as incoming ligands particularly depends on σ effects, π effects, and steric effects. We note that the two most reactive solvents Me_2CO and MeCN are also the most π acidic; among these, MeCN is the least basic.

V. Ligand-Exchange Reactions of $\text{TpRu}(\text{CO})_2(\text{L})^+\text{PF}_6^-$. In order to assess in a qualitative manner the relative strength of binding of the ligands L at the $\text{TpRu}(\text{CO})_2^+$ moiety for the series $\text{L} = \text{MeCN}$, THF , Me_2CO , and H_2O , ligand-exchange reactions were investigated by ^1H NMR spectroscopy in nitromethane- d_3 . The ^1H NMR spectroscopic data for the Tp region of all relevant compounds are listed in Table 1.

The addition of 10 equiv of D_2O to $\text{TpRu}(\text{CO})_2(\text{Me}_2\text{CO})^+$ (4) resulted in rapid and quantitative conversion to $\text{TpRu}(\text{CO})_2(\text{D}_2\text{O})^+$ (5- d_2), as evidenced by the replacement of the Tp resonances of 4 by those of 5. Analogous experiments in which 10 equiv of the incoming ligand was added established the replacement of acetone by THF- d_8 and acetonitrile- d_3 , of THF

Scheme 2

by acetonitrile- d_3 and D_2O , and of water by acetonitrile- d_3 . The observed ligand-exchange reactions are summarized in Scheme 2, and the results establish that the strength of metal–ligand binding decreases in the order $\text{MeCN} > \text{H}_2\text{O} > \text{THF} > \text{Me}_2\text{CO}$. The order is different from the ordering of the reaction rates. The fact that the binding of MeCN is strongest is expected on the basis of ligand bond energy data for a large number of complexes; THF and Me_2CO often have quite similar ligand–metal bond strengths.¹⁹ For the MeCN , THF , and Me_2CO complexes, the order of stabilities is different from that of the rates of reaction of the solvents. We find it somewhat surprising that MeCN , usually²⁰ considered to be a good ligand and thus a reactive solvent, is not superior to the poorer ligand Me_2CO in kinetic terms.

Summary. Oxidative cleavage of metal–metal bonded dimer of Tp-bonded metals has been employed for the preparation of new monomeric cationic complexes. The weak bonding in the easily prepared THF adduct should make this complex a prime precursor for the future synthesis of novel Tp–ruthenium complexes. During the course of the present work, it has been established that the solvent can be directly involved and assist on a molecular level in the oxidative cleavage of metal–metal bonded dimers. The bimolecular nature of the reactions cause these to bear resemblance to ligand-substitution reactions at mononuclear 17-electron species, which are usually associative in nature.

Experimental Section

General Procedures. All manipulations involving organometallic compounds were carried out with use of vacuum line, Schlenk, syringe, or drybox techniques. Acetonitrile was distilled from P_2O_5 , and acetonitrile- d_3 , dichloromethane, and dichloromethane- d_2 were distilled from CaH_2 . Acetone was freshly distilled from K_2CO_3 . THF was distilled from sodium benzophenone ketyl. Nitromethane- d_3 was distilled from CaCl_2 . Acetonitrile and dichloromethane containing the supporting electrolyte were passed through a column of active neutral alumina prior to use to remove water and protic impurities before electrochemical measurements. The electrolyte was freed of air by purging with purified solvent-saturated argon, and all measurements and electrolyses were carried out under a blanket of argon.

Electrochemical Measurements. Electrochemical measurements were performed with an EG&G-PAR Model 273 potentiostat/galvanostat driven by an external HP 3314A sweep generator. The signals were fed to a Nicolet 310 digital oscilloscope and processed by an on-line personal computer. The working electrode was a Pt disk electrode ($d = 0.6$ mm), the counter electrode was a Pt wire, and the Ag wire reference electrode assembly^{21a} was filled with acetonitrile/0.01 M AgNO_3 /0.1 M $\text{Bu}_4\text{N}^+\text{PF}_6^-$. The reference electrode was calibrated against Cp_2Fe which is also used as the reference in this work. Positive-feedback iR compensation was employed; the separation

(19) Hoff, C. D. *Prog. Inorg. Chem.* **1992**, *40*, 503.

(20) Crabtree, R. H. *The Organometallic Chemistry of Transition Metals*, 2nd ed.; Wiley: New York, 1994.

(21) (a) Moe, N. S. *Anal. Chem.* **1974**, *46*, 968. (b) Ahlberg, E.; Parker, V. D. *J. Electroanal. Chem. Interfacial Electrochem.* **1981**, *121*, 57. (c) Ahlberg, E.; Parker, V. D. *Acta Chem. Scand., Ser. B* **1980**, *B34*, 97.

(17) Tyler, D. R. In *Organometallic Radical Processes*; Troglor, W. C., Ed.; Elsevier: Amsterdam, 1990; p 338 and references cited.

(18) Gutmann, V. *Coord. Chem. Rev.* **1976**, *18*, 225.

of anodic and cathodic peaks for the Cp_2Fe oxidation was 59–61 mV in acetonitrile at 20 °C. Data-handling procedures for the DCV analysis have been described previously.^{14b,21b,c} For measurement series involving large changes in temperature T or concentrations c , the choice of performing $\nu_{0.5}$ or $\nu_{0.6}$ measurements was made such as to achieve the most convenient sweep rate (not too slow due to electrode size; not too large due to incomplete iR compensation in some cases) over the whole range of T or c .

^1H and $^{13}\text{C}\{^1\text{H}\}$ NMR spectra were recorded on Varian XL-300 and Varian Gemini-200 instruments. Chemical shifts are reported in ppm relative to tetramethylsilane, with the solvent residual proton (^1H) or carbon (^{13}C) resonances as internal standards. Infrared spectra were obtained on a Perkin-Elmer 1310 infrared spectrophotometer. Melting points were measured on a Büchi melting point apparatus in capillary tubes sealed under vacuum. Elemental analyses were performed by Ilse Beetz Mikroanalytisches Laboratorium, Kronach, Germany.

The compounds $\text{Tp}_2\text{Ru}_2(\text{CO})_4$,^{8a} $\text{Cp}_2\text{Fe}^+\text{PF}_6^-$,^{22a} and $\text{Cp}_2\text{Ru}_2(\text{CO})_4$ ^{22b} were prepared according to published procedures.

$\text{TpRu}(\text{CO})_2(\text{NCMe})^+\text{PF}_6^-$ (2**(PF_6^-)).** $\text{Cp}_2\text{Fe}^+\text{PF}_6^-$ (43 mg, 0.13 mmol) was added to a stirred solution of **1** (51 mg, 0.069 mmol) in acetonitrile (5 mL) at ambient temperature. The blue color of the oxidant gradually faded, and after 16 h, the solvent was concentrated by vacuum transfer. The crude product was precipitated as a grayish powder by the addition of ether and washed repeatedly with ether. The solid was dissolved in acetonitrile, the solution was filtered through Celite, and the product (43 mg, 60%) was crystallized by the slow addition of ether: mp 235–240 °C dec; ^1H NMR (acetonitrile- d_3) δ 2.42 (s, 3 H), 6.36 (dd, $J = 2.2, 2.4$ Hz, 1 H), 6.45 (dd, $J = 2.0, 2.6$ Hz, 1 H), 7.87 (d, $J = 2.2$ Hz, 1 H), 7.89 (d, $J = 2.8$ Hz, 1 H), 7.93 (d, $J = 2.8$ Hz, 2 H), 8.06 (d, $J = 2.2$ Hz, 2 H); $^{13}\text{C}\{^1\text{H}\}$ NMR (acetonitrile- d_3) δ 4.7 (CH_3CN), 107.1, 107.6 (Tp), 127.9 (CH_3CN), 136.5, 137.5 (Tp), 143.6, 146.2 (Tp), 189.7 (CO); IR (acetonitrile) ν_{CO} 2045, 2095 cm^{-1} . Anal. Calcd for $\text{C}_{13}\text{H}_{13}\text{BF}_6\text{N}_7\text{O}_2\text{PRu}$: C, 28.08; H, 2.36; N, 17.63. Found: C, 28.63; H, 2.35; N, 17.55.

$\text{TpRu}(\text{CO})_2(\text{THF})^+\text{PF}_6^-$ (3**(PF_6^-)).** A mixture of $\text{Cp}_2\text{Fe}^+\text{PF}_6^-$ (70 mg, 0.21 mmol) and **1** (100 mg, 0.135 mmol) was stirred in THF (5 mL) for 16 h at ambient temperature. The blue color of the oxidant gradually faded, and grayish white microcrystals precipitated. The solvent was decanted, and the solid was washed repeatedly with ether. The solid was dissolved in dichloromethane, and the product (88 mg, 71%) was crystallized by the slow addition of ether: mp 178–183 °C dec; ^1H NMR (dichloromethane- d_2) δ 2.01 (m, 4 H, THF), 3.72 (m, 4 H, THF), 6.33 (t, $J = 2.2$ Hz, 1 H), 6.54 (t, $J = 2.2$ Hz, 2 H), 7.50 (d, $J = 2.2$ Hz, 1 H), 7.81 (d, $J = 2.6$ Hz, 1 H), 7.95 (d, $J = 2.2$ Hz, 2 H), 7.99 (d, $J = 1.8$ Hz, 2 H); $^{13}\text{C}\{^1\text{H}\}$ NMR (dichloromethane- d_2) δ 26.6 (THF), 79.3 (THF), 108.8, 109.1, 138.2, 139.3, 144.6, 147.7 (Tp), 192.7 (CO); IR (dichloromethane) ν_{CO} 2024, 2084 cm^{-1} . Anal. Calcd for $\text{C}_{15}\text{H}_{18}\text{BF}_6\text{N}_6\text{O}_3\text{PRu}$: C, 30.68; H, 3.09; N, 14.31. Found: C, 29.99; H, 3.04; N, 14.31.

$\text{TpRu}(\text{CO})_2(\text{Me}_2\text{CO})^+\text{PF}_6^-$ (4**(PF_6^-)).** $\text{Cp}_2\text{Fe}^+\text{PF}_6^-$ (49 mg, 0.15 mmol) was added to a stirred solution of **1** (64 mg, 0.086 mmol) in

acetone (5 mL) at ambient temperature, and the solution was stirred for 16 h. The solution was concentrated by vacuum transfer. The product was precipitated as a grayish powder by the addition of ether and washed repeatedly with ether. The solid was dissolved in acetone, the solution was filtered through Celite, and the product (45 mg, 52%) was crystallized by the slow addition of ether: mp 175–179 °C dec; ^1H NMR (nitromethane- d_3) δ 2.65 (s, 6 H), 6.44 (t, $J = 2.5$ Hz, 1 H), 6.50 (t, $J = 2.4$ Hz, 2 H), 7.85 (d, $J = 2.2$ Hz, 1 H), 7.93 (d, $J = 2.1$ Hz, 2 H), 8.01 (d, $J = 2.6$ Hz, 1 H), 8.03 (d, $J = 2.5$ Hz, 2 H); $^{13}\text{C}\{^1\text{H}\}$ NMR (90:10 acetone/acetone- d_6) δ 33.3 (Me_2CO), 108.2, 109.2, 138.0, 139.7, 144.6, 148.5 (Tp), 193.7 (CO), 205.6 (Me_2CO); IR (dichloromethane) ν_{CO} 2024, 2084 cm^{-1} .

$\text{TpRu}(\text{CO})_2(\text{H}_2\text{O})^+\text{PF}_6^-$ (5**(PF_6^-)).** $\text{Cp}_2\text{Fe}^+\text{PF}_6^-$ (63 mg, 0.19 mmol) and **1** (75 mg, 0.10 mmol) were added to a dichloromethane (5 mL)/water (10 mL) mixture, and the mixture was vigorously stirred for 12 h at ambient temperature. Grayish white crystals precipitated. The solvent was decanted, and the solid was washed repeatedly with ether. The material was dissolved in dichloromethane, and the product (56 mg, 52%) was crystallized by the slow addition of ether: mp 174–176 °C dec; ^1H NMR (nitromethane- d_3) δ 6.39 (t, $J = 2.4$ Hz, 1 H), 6.51 (t, $J = 2.3$ Hz, 2 H), 7.77 (d, $J = 2.2$ Hz, 1 H), 7.95 (d, $J = 2.0$ Hz, 1 H), 8.03 (d, $J = 2.7$ Hz, 2 H), 8.05 (d, $J = 2.2$ Hz, 2 H); IR (dichloromethane) ν_{CO} 2026, 2084 cm^{-1} .

$\text{CpRu}(\text{CO})_2(\text{NCMe})^+\text{PF}_6^-$. A mixture of $\text{Cp}_2\text{Ru}_2(\text{CO})_4$ (50 mg, 0.11 mmol) and $\text{Cp}_2\text{Fe}^+\text{PF}_6^-$ (70 mg, 0.21 mmol) was stirred in acetonitrile (5 mL) for 5 h at ambient temperature. The solution was concentrated by vacuum transfer. Off-white crystals were precipitated by the addition of ether. The solid was washed with ether and dissolved in acetonitrile, and the product (25 mg, 30%) was crystallized by slow addition of ether: mp 140–142 °C; ^1H NMR (acetonitrile- d_3) δ 2.34 (s, 3 H), 5.65 (s, 5 H); $^{13}\text{C}\{^1\text{H}\}$ NMR (acetonitrile- d_3) δ 4.7 (MeCN), 89.1 (Cp), 194.4 (CO). Anal. Calcd for $\text{C}_9\text{H}_8\text{F}_6\text{NO}_3\text{PRu}$: C, 26.48; H, 1.98; N, 3.43. Found: C, 26.38; H, 2.34; N, 3.92.

Constant-Potential Coulometry Measurements. Constant-potential coulometry measurements were performed in an H-shaped cell, the compartments of which were separated by a medium-frit glass junction. A platinum-gauze working electrode was used. Solutions of 10–20 mg of substrate in 20 mL of solvent/supporting electrolyte were electrolyzed at the oxidation peak potential of the cyclic voltammograms. $\text{Bu}_4\text{N}^+\text{PF}_6^-$ was employed as the supporting electrolyte (0.1 M in acetonitrile, 0.2 M in THF and acetone). Three separate measurements were made for each compound in each solvent.

For the purpose of product identification, electrolyses were performed on solutions with $\text{Me}_4\text{N}^+\text{BF}_4^-$ as the supporting electrolyte. After electrolysis, the solvent was removed in vacuo and the remaining solvent was extracted with dichloromethane. The solution was filtered, the solvent was removed, and the products were identified by ^1H NMR spectroscopy of the crude mixture.

Acknowledgment. We acknowledge generous support from Statoil under the VISTA program, administered by the Norwegian Academy of Science and Letters.

(22) (a) Lyatifov, I. R.; Solodovnikov, S. P.; Babin, V. N.; Materikova, R. B. *Z. Naturforsch., B* **1979**, *34B*, 863. (b) Humphries, A. P.; Knox, S. A. R. *J. Chem. Soc., Dalton Trans.* **1975**, 1710.